# Transceiver Design for AF MIMO Relay Systems With a Power Splitting Based Energy Harvesting Relay Node

Bin Li, *Senior Member, IEEE*, Meiying Zhang, Hanyu Cao, Yue Rong, *Senior Member, IEEE*, and Zhu Han, *Fellow, IEEE*

***Abstract*—In this article, a dual-hop amplify-and-forward (AF) multiple-input multiple-output (MIMO) relay communication system is studied. With a splitting (PS) protocol, the relay node harvests the radio frequency (RF) energy in the signals sent by the source node and utilizes the harvested energy to forward signals from the source node to the destination node. We aim at maximizing the source-destination mutual information (MI) through a joint design of the source matrix, the relay matrix, and the PS ratios under the source node power constraint and the relay node harvested energy constraint. We consider a general sum energy constraint at the relay node with different PS ratios across relay antennas, which includes existing works based on uniform PS or per data stream energy constraint as special cases. Moreover, a practical nonlinear energy harvesting (EH) model is adopted, where the harvested energy is bounded as the incident RF signal power increases. We establish the structure of the source matrix and the relay matrix, which simplifies the complicated transceiver design problem with matrix variables to a power distribution problem with scalar variables. Three approaches are proposed to efficiently solve the optimal power distribution problem. In particular, the first proposed algorithm solves the original nonconvex power allocation problem using the sequential quadratic programming, while the other two algorithms convert the original problem to convex problems by exploiting a tight upper bound and a tight lower bound of the objective function, respectively. Numerical simulations demonstrate that when the EH circuit works in the linear region, the proposed algorithms have a larger system MI than existing PS and TS based MIMO AF relay systems. The peak harvest power constraint plays an important role in choosing the location of the relay node.**

***Index Terms*—Energy harvesting, power splitting receiver, multiple-input multiple-output relay, amplify-and-forward relay.**

Manuscript received June 14, 2019; revised October 9, 2019 and November 26, 2019; accepted December 31, 2019. Date of publication January 6, 2020; date of current version March 12, 2020. This work was supported in part by the National Natural Science Foundation of China under Grant 61701124, in part by the Sichuan Science and Technology Program under Grant 2019YJ0105, in part by the Fundamental Research Funds for the Central Universities (China), and in part by US MURI AFOSR MURI 18RT0073,\penalty -\@M NSF EARS-1839818, CNS-1717454, CNS-1731424, CNS-1702850, and CNS-1646607. The review of this article was coordinated by Prof. Q. Song. *(Corresponding author: Yue Rong.)*

B. Li is with the College of Electrical Engineering and the Key Laboratory of Wireless Power Transmission of Ministry of Education, Sichuan University, Chengdu 610017, China (e-mail: bin.li@scu.edu.cn).

M. Zhang and H. Cao are with the College of Electrical Engineering, Sichuan University, Chengdu 610017, China (e-mail: mei.ying.zhang@hotmail.com; jasontsow@gmail.com).

Y. Rong is with the School of Electrical Engineering, Computing and Mathematical Sciences, Curtin University, Perth, WA 6845, Australia (e-mail: y.rong@curtin.edu.au).

Z. Han is with the University of Houston, Houston, TX 77004 USA, and also with the Department of Computer Science and Engineering, Kyung Hee University, Seoul 446-701, South Korea (e-mail: zhan2@uh.edu).

Digital Object Identifier 10.1109/TVT.2020.2964069

## I. Introduction

### A. Background

THE number of wireless devices has significant increased over the last years. A key factor which limits the performance of these devices is the life time and energy constraints. The life time of these devices can be extended by battery replacing. However, battery replacing may be costly and hard to perform in many cases because of physical or economic constraints. For example, for some applications wireless devices can be located inside building structures or human bodies.

Thus, it is important for wireless systems to have the capability of harvesting energy from external sources [1]. Conventional energy harvesting (EH) technologies, which mainly rely on natural energy resources such as solar energy and wind, have drawbacks in that these energy sources are hard to control. Thus, they do not provide a reliable power supply to wireless devices. In order to overcome the constraints of conventional EH methods, an emerging technology utilizing radio frequency (RF) signals to transfer energy has been proposed [2]. Compared with conventional EH technologies, the RF-based EH and wireless powered communication (WPC) technique has distinct advantages for wireless networks.

### B. Related Works

In [3], an ideal receiver which performs simultaneous information decoding (ID) and EH has been discussed. However, this ideal receiver has two challenges for practical implementation [2]. Firstly, circuits aimed for EH usually cannot decode the information carried by the signal. To coordinate wireless information transmission (WIT) and wireless energy transfer (WET), time switching (TS) and power splitting (PS) protocols have been developed in [4]. Secondly, as WIT and WET systems work with different sensitivity ($-60$ dBm and $-10$ dBm for ID receivers and EH receivers, respectively), the architecture of traditional ID receivers may not be optimal for the EH receivers.

To overcome this limit, in [2] separated and integrated structure receivers have been proposed for a more general dynamic PS protocol. Waveform design for efficient WET has been studied in [5] and [6].

Multiple-input multiple-output (MIMO) technology can increase the system spectral efficiency and energy efficiency [7]–[9]. Moreover, by installing multiple transmit antennas at nodes of a wireless network, RF energy can be more effectively delivered to wireless devices compared with nodes having only a single antenna, and thus, the life time of energy limited wireless systems is effectively extended. A MIMO broadcasting system using a receiver with separated ID and EH architecture has been proposed in [4], where the rate-energy regions have been calculated for the PS and TS protocols. A multiple-input single-output (MISO) system has been investigated in [10], where under signal-to-interference-plus-noise ratio (SINR) constraints, joint design of the transmit beamforming vector and the PS ratio is performed to minimize the total transmission power.

Relay technique can be used to expand the network coverage of wireless communication [11]–[13]. In relay systems with EH relays, relay nodes can harvest RF energy and receive information from the source node. Then the relay nodes process and forward the source signals to the destination nodes by utilizing the harvested RF energy. Recently, employment of EH relay nodes in relay systems has been studied in [14]–[21]. PS and TS based EH protocols have been studied in [14] with amplify-and-forward (AF) relay systems. In [15], a cooperative system has been proposed, where multiple transmitter-receiver pairs communicate simultaneously under the assistance of an EH relay node. The effect of the distribution of user energy on the system performance and complexity has been studied in [15]. A communication system with randomly placed decode-and-forward (DF) wireless powered relays has been addressed in [16]. The authors of [16] have shown that the same diversity gain as traditional relay nodes with constant power supply can be achieved with EH relays. For WPC in interference relay networks, a game theoretic distributed PS approach has been developed in [17]. In [18], WPC for a relay system with the orthogonal frequency-division multiplexing technology has been studied. Recently, WPC using full duplex relays has been studied in [19]–[21].

The employment of EH relays in MIMO relay communication systems has been discussed in [22]–[32]. Under several receiver architectures, energy-rate trade-offs by applying the EH technique in MIMO relay communication systems have been investigated in [22]. Challenges in this research topic have also been presented in [22]. PS and TS protocols have been proposed in [23] for an AF MIMO relay communication system, where the joint source matrix and relay matrix optimization has been considered to optimize the system rate. In particular, per data stream energy constraint has been considered for the PS protocol in [23]. An AF MIMO relay communication system based on space-time block code and an EH receiver with multiple antennas has been investigated in [24] and [25], where joint source matrix and relay matrix optimization has been proposed to achieve energy-rate trade-offs.

In [26], WPC has been applied in massive MIMO relay systems. In [27], the relay matrix optimization has been investigated for a relay system with a multi-antenna EH relay node and single-antenna source and destination nodes. An iterative algorithm and a channel diagonalization base algorithm have been developed in [28] for the joint optimization of the relay matrix and the source precoder in wireless-powered MIMO relay networks. Iterative approaches and dual decomposition have been proposed in [29] for MIMO relay systems with a PS-based EH relay. Recently, joint transceiver optimization for wireless information and energy transfer in AF MIMO relay systems has been studied in [30], where a general source node energy consumption constraint has been considered.

### C. Contributions of This Paper

In this work, we study a dual-hop AF MIMO relay communication system, where a receiver with EH capability is applied at the relay to facilitate the information and energy transmission. The relay node is particularly useful in systems where the direct source-destination link is much weaker than the link through the relay node due to shadowing and path attenuation by obstacles [23]–[25], [29], [30]. We apply the PS protocol in this paper, where signals received at the relay node are split into two portions. One part of the signals are linearly precoded and forwarded to the destination node using the energy harvested from the other part of the signals.

It is assumed in [23] that the energy harvested on one subchannel of the source-relay link is solely used for transmitting the information on this subchannel. Here, we depart from this strict per data stream energy constraint and consider a general sum energy constraint at the relay node. Compared to the formulation in [23], the total energy harvested by the relay node over all antennas can be used to forward signals at all subchannels. Thus, the sum energy constraint in this paper is more general and includes the per data stream energy constraints adopted in [23] as special cases. Therefore, we can expect a better system performance.

We would also like to note that in [26]–[29], the same PS ratio is applied across all antennas (i.e., uniform PS according to [4]). On the contrary, in this paper we consider a more general system with different PS ratios across antennas. Since the proposed system includes the uniform PS ratio systems [26]–[29] as a special case, a better system performance can be achieved. On the other hand, the system optimization problem is more challenging to solve, as multiple PS ratios need to be optimized. For systems where the same PS ratio is used across all antennas (e.g. [28]), an exhaustive search is applied to optimize the PS ratio, which can be time-consuming if a very small step-size is adopted during the search. With multiple PS ratios, the optimization method needs to be changed, as it is impractical to use exhaustive search over multiple dimensions.

In [22]–[30], it is assumed that the harvested power at the relay node linearly increases with the power of the incident RF signal. However, it has been shown in [33], [34] that such linear model does not hold in practice. In this paper, a practical nonlinear EH

model is adopted, where the harvested energy is bounded as the incident RF signal power increases.

We investigate the joint design of the source matrix, the relay matrix, and the PS ratios to optimize the achievable system mutual information (MI), under the power constraint at the source node and the proposed sum harvested energy constraint at the relay node. We derive the structure of the source matrix and the relay matrix, which reduces the complex-valued matrix optimization variables to scalar power allocation optimization variables. We propose three approaches to efficiently solve the optimal power distribution problem. In particular, the first proposed algorithm solves the original nonconvex power allocation problem using the sequential quadratic programming (SQP) method [35], while the other two algorithms convert the original problem to convex problems by utilizing a tight upper bound and a tight lower bound of the system MI function, respectively. In particular, we demonstrate that the optimal power allocation problem based on the upper bound can be converted to a nonlinear semidefinite programming (SDP) problem, which can be efficiently solved by the disciplined convex programming toolbox CVX [36]. A primal-dual interior-point method is applied to solve the lower bound based power distribution problem. We demonstrate through numerical simulations that the three proposed algorithms have a very similar performance in terms of the system MI.

The main contributions of this paper compared with the state-of-the-art approaches are summarized as follows:

1) Compared with [26]–[29], a more general system with different PS ratios across antennas is considered in this paper.
2) A general sum energy constraint is proposed at the relay node compared with the per data stream energy constraint in [23]. Based on our best knowledge, this has not been considered in the literature when different PS ratios are used across relay antennas. The sum energy constraint enables a more flexible allocation of the harvested energy to the concurrent data streams at the relay node.
3) Compared with [22]–[30], a more practical nonlinear EH model is adopted at the relay node. In addition, the circuit energy consumption has been considered at the relay node.
4) By exploiting the structure of the source matrix and the relay matrix, the difficult joint transceiver design problem is reduced to a simpler optimal power allocation problem.
5) Three algorithms are developed to solve the optimal source and relay power allocation problem. These algorithms achieve complexity-performance trade-offs. In particular, the third algorithm yields a slightly smaller system MI with a lower computational complexity compared with the first two algorithms.
6) The proposed algorithms are shown to yield higher system MI than that in [23], [29], and [30] when the EH works in the linear range.

The system and algorithms developed in this paper can be applied, for example, in a heterogeneous wireless network which consists of users of various capabilities. Inactive users having MIMO capabilities in the network can be utilized as relay nodes to assist those active users [22]. In particular, by harvesting the RF energy transmitted by the access point, these relay nodes do not need to use their own energy supply to help forwarding signals from the access point to the destination node. This would help motivate users to be involved in the relay system. It is known that the EH nonlinear response is a function of the input signal properties, i.e. shape, and not only power, as shown in [5] and [6]. However, in this paper, only the dependence on the input power is modeled, and there is therefore no claim of optimality on the transmit signal.

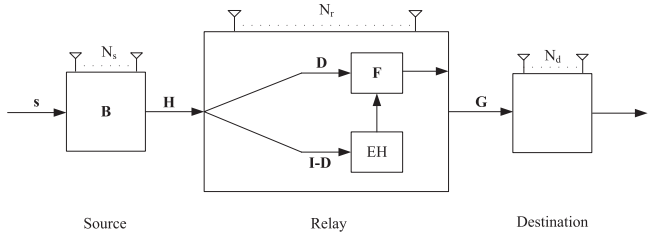


Fig. 1. A dual-hop AF MIMO relay system with a PS based EH relay node.

### D. Organization

The remainder of this article is organized as below. The system model of a dual-hop AF MIMO relay system employing a wireless powered relay node is introduced in Section II. The joint source, relay, and PS ratio optimization problem is also formulated in this section. In Section III, three algorithms are presented to solve the source and relay design problem. Numerical simulations are performed in Section IV to compare the performance of existing approaches with our proposed transceiver design algorithms. Finally, we draw conclusions in Section V.

## II. System Model

We investigate a dual-hop three-node MIMO communication system where a source node communicates with a destination node via a relay node as illustrated in Fig. 1. The number of antennas at the source, relay, and destination nodes are $N_s$, $N_r$, and $N_d$, respectively. It is assumed that both the source node and the destination node have constant power supply, but the relay node obtains its power from harvesting the RF energy from signals sent from the source node. One source-destination communication cycle is completed in two phases with equal duration. During the source phase, energy and information carrying signals are sent from the source node to the relay node, and the relay node adopts the PS protocol [4] to harvest energy from the received signals.

For the relay phase, the information-bearing signals received by the relay node are multiplied by a precoding matrix and forwarded to the destination node [23]. Among various relay protocols at the relay node, we choose the AF scheme thanks to its shorter processing delay and implementation simplicity. Moreover, in contrast to regenerative relay protocols, in the AF relay protocol, the relay node does not need to decode and then re-encode information signals. Thus, the amount of signal processing and coding work at the relay node is smaller in an AF relay system. This reduces the power consumption of the relay

node and makes the AF scheme suitable for wireless-powered relay nodes. Following [23]–[25], [29], and [30], the direct link between the source node and the destination node is omitted, as compared with the link through the relay node, path shadowing and attenuation are more severe on the direct link. This is a typical scenario where relay nodes are useful. If there exists a strong direct link, it is better to have a one-hop source-destination communication through the direct path.

During the source phase with a duration of $T/2$, where $T$ is the duration of one source-destination communication cycle, an $N_s \times 1$ source signal vector $\mathbf{s}$ is multiplied by an $N_s \times N_s$ source matrix $\mathbf{B}$. Then the precoded vector is sent to the relay node. We assume that $E\{\mathbf{s}\mathbf{s}^H\} = \mathbf{I}_{N_s}$, where $E\{\cdot\}$ is the statistical expectation, $\mathbf{I}_n$ stands for an $n \times n$ identity matrix, and $(\cdot)^H$ represents the Hermitian transpose. For the sake of notational simplicity, we choose $T = 2$ in the rest of the paper. The signal vector received by the relay node is given by

$$\mathbf{y}_r = \mathbf{H}\mathbf{B}\mathbf{s} + \mathbf{v}_a \tag{1}$$

where $\mathbf{H}$ is an $N_r \times N_s$ MIMO channel matrix between the source and relay nodes, and $\mathbf{v}_a$ is the noise at the antenna.

During the relay phase with a duration of $T/2 = 1$, with the PS protocol, the relay node first applies $d_i \geq 0$ to split $y_{r,i}$, where $y_{r,i}$ is the received signal at the $i$th antenna of the relay node. Then $\sqrt{d_i}\, y_{r,i}$ is used for information transmission and $\sqrt{1-d_i}\, y_{r,i}$ is reserved for EH. From (1), the information-bearing signal vector $\mathbf{y}_i$ and the energy-carrying signal vector $\mathbf{y}_e$ can be written respectively as

$$\mathbf{y}_i = \mathbf{D}^{\frac{1}{2}}\mathbf{y}_r + \mathbf{v}_r = \mathbf{D}^{\frac{1}{2}}\mathbf{H}\mathbf{B}\mathbf{s} + \mathbf{D}^{\frac{1}{2}}\mathbf{v}_a + \mathbf{v}_r \tag{2}$$

$$\mathbf{y}_e = (\mathbf{I}_{N_r} - \mathbf{D})^{\frac{1}{2}}\mathbf{y}_r = (\mathbf{I}_{N_r} - \mathbf{D})^{\frac{1}{2}}\mathbf{H}\mathbf{B}\mathbf{s} + (\mathbf{I}_{N_r} - \mathbf{D})^{\frac{1}{2}}\mathbf{v}_a \tag{3}$$

where $\mathbf{D} = \mathrm{diag}(d_1, \ldots, d_{N_r})$ is the $N_r \times N_r$ diagonal PS matrix, $\mathbf{v}_r$ is the noise vector introduced by the RF to baseband signal conversion [4] at the relay node with zero-mean and $E\{\mathbf{v}_r\mathbf{v}_r^H\} = \sigma_r^2\mathbf{I}_{N_r}$. Here $\mathrm{diag}(\cdot)$ stands for a diagonal matrix. Similar to [2], we assume that $\mathbf{v}_r$ is much larger than $\mathbf{v}_a$ and the energy in $\mathbf{v}_a$ is much smaller than that in $\mathbf{H}\mathbf{B}\mathbf{s}$. Therefore, (2) and (3) can be approximated by

$$\mathbf{y}_i \approx \mathbf{D}^{\frac{1}{2}}\mathbf{H}\mathbf{B}\mathbf{s} + \mathbf{v}_r \tag{4}$$

$$\mathbf{y}_e \approx (\mathbf{I}_{N_r} - \mathbf{D})^{\frac{1}{2}}\mathbf{H}\mathbf{B}\mathbf{s}. \tag{5}$$

With a linear EH model (e.g. [23] and [26]–[30]), the RF energy harvested by the relay node can be obtained from (5) as

$$\begin{aligned} E_r' &= \eta_1 E\{\mathrm{tr}(\mathbf{y}_e\mathbf{y}_e^H)\} \\ &= \eta_1 \mathrm{tr}((\mathbf{I}_{N_r} - \mathbf{D})\mathbf{H}\mathbf{B}\mathbf{B}^H\mathbf{H}^H) \end{aligned} \tag{6}$$

where $0 < \eta_1 < 1$ denotes the efficiency of energy conversion and $\mathrm{tr}(\cdot)$ stands for the matrix trace. It has been shown in [33] and [34] that the linear model (6) is optimistic and for practical EH circuits, the harvested energy is bounded as the incident RF signal power increases. Taking this upper-bound into account, we apply the following nonlinear EH model[1] [37]–[39]

$$E_r = \min(\eta_1 \mathrm{tr}((\mathbf{I}_{N_r} - \mathbf{D})\mathbf{H}\mathbf{B}\mathbf{B}^H\mathbf{H}^H), E_m') \tag{7}$$

where $E_m'$ is the maximum output power of the EH circuit when it is saturated [33]. Since $T/2 = 1$, $E_m'$ is also the maximal harvested energy at the relay node.[2]

From (4), the signal vector transmitted by the relay node is given by

$$\mathbf{x}_r = \mathbf{F}\mathbf{y}_i = \mathbf{F}\mathbf{D}^{\frac{1}{2}}\mathbf{H}\mathbf{B}\mathbf{s} + \mathbf{F}\mathbf{v}_r \tag{8}$$

where $\mathbf{F}$ is an $N_r \times N_r$ linear precoding matrix at the relay node. Based on (8), the signal vector received at the destination node can be written as

$$\begin{aligned} \mathbf{y}_d &= \mathbf{G}\mathbf{x}_r + \mathbf{v}_d \\ &= \mathbf{G}\mathbf{F}\mathbf{D}^{\frac{1}{2}}\mathbf{H}\mathbf{B}\mathbf{s} + \mathbf{G}\mathbf{F}\mathbf{v}_r + \mathbf{v}_d \end{aligned} \tag{9}$$

where $\mathbf{G}$ is an $N_d \times N_r$ MIMO channel matrix between the relay and destination nodes, and $\mathbf{v}_d$ is the AWGN vector at the destination node with zero-mean and $E\{\mathbf{v}_d\mathbf{v}_d^H\} = \sigma_d^2\mathbf{I}_{N_d}$. From (9), the MI between the source and destination nodes can be written as [11]

$$\begin{aligned} \mathrm{MI}(\mathbf{D}, \mathbf{Q}, \mathbf{F}) = \frac{1}{2}\log \Big| &\mathbf{I}_{N_d} + \mathbf{G}\mathbf{F}\mathbf{D}^{\frac{1}{2}}\mathbf{H}\mathbf{Q}\mathbf{H}^H\mathbf{D}^{\frac{1}{2}}\mathbf{F}^H\mathbf{G}^H \\ &\times \left(\sigma_r^2\mathbf{G}\mathbf{F}\mathbf{F}^H\mathbf{G}^H + \sigma_d^2\mathbf{I}_{N_d}\right)^{-1} \Big| \end{aligned} \tag{10}$$

where $\mathbf{Q} = \mathbf{B}\mathbf{B}^H$, $(\cdot)^{-1}$ and $|\cdot|$ stand for the matrix inversion and matrix determinant, respectively.

It is assumed that channel matrices $\mathbf{H}$ and $\mathbf{G}$ are quasi-static block fading which are constant over some time before they change to another realization. We assume that the channel state information (CSI) of $\mathbf{H}$ and $\mathbf{G}$ is known. In practice, the required CSI can be estimated, for instance, through algorithms in [50] and the references therein. From (8), the energy consumption at the relay node to forward $\mathbf{x}_r$ to the destination node is represented as

$$\mathrm{tr}\left(E\left\{\mathbf{x}_r\mathbf{x}_r^H\right\}\right) = \mathrm{tr}\left(\mathbf{F}\left(\mathbf{D}^{\frac{1}{2}}\mathbf{H}\mathbf{Q}\mathbf{H}^H\mathbf{D}^{\frac{1}{2}} + \sigma_r^2\mathbf{I}_{N_r}\right)\mathbf{F}^H\right). \tag{11}$$

[1] Besides the saturation nonlinear model [37]–[39], there are other nonlinear models such as [5], [6], [40], [41] which is based on the diode current analysis, and [33], [34], [42] which is based on curve-fitting of the input-output power. In particular, fitting methods to model nonlinearity in a larger range of input power are available in [42]. It is shown in [5] and [6] that the EH efficiency is dependent on the waveform of the input signal, which has an impact on the amount of harvested power, particularly in the low power regime. For the saturation nonlinear model, it is shown in [43] and [44] that transmit signal (modulation, input distribution, etc) needs to be optimized to account for nonlinearity. Among various nonlinear models, the model in [37]–[39] is analytically tractable for the AF MIMO relay system considered in this paper and is shown to match the experimental results [39].

[2] Saturation of the EH circuits has been observed in experimental results [45]–[47]. The reason of the saturation effect is that when a diode is reverse biased by a voltage higher than its breakdown voltage, the diode operates at its breakdown region. Therefore, the output power of the EH circuit is limited by the diode breakdown voltage [40], [41]. In practical systems, the harvester should avoid working in the saturation region, which can be achieved by designing the harvester correctly as explained in [40, Remark 5] and [41, Table 1]. In this work, the saturation effect of the EH circuits is considered for the generality of analysis. It will be shown that the saturation nonlinear model plays an important role in choosing the location of the relay node.

Following [51], we consider the circuit energy consumption at the relay node, which consists of a static part for the basic consumption of the circuit and a dynamic part that varies with the amount of information transmission. The static part is modeled as $N_r P_c$, where $P_c$ denotes the power consumption of the circuit driving each antenna. The dynamic part is given by $\xi E_r$, where $0 < \xi < 1$ [30]. According to (7) and (11), the energy constraint at the relay node is given by

$$\mathrm{tr}\left(\mathbf{F}\left(\mathbf{D}^{\frac{1}{2}}\mathbf{H}\mathbf{Q}\mathbf{H}^H\mathbf{D}^{\frac{1}{2}} + \sigma_r^2\mathbf{I}_{N_r}\right)\mathbf{F}^H\right) + N_r P_c \le (1-\xi)E_r. \tag{12}$$

From (10) and (12), the transceiver optimization problem for the proposed AF MIMO relay system with a PS based EH relay node can be written as,[3]

$$\max_{\mathbf{D},\mathbf{Q},\mathbf{F}} \quad \mathrm{MI}(\mathbf{D},\mathbf{Q},\mathbf{F}) \tag{13a}$$

$$\text{s.t.} \quad \mathrm{tr}(\mathbf{Q}) \le P \tag{13b}$$

$$\mathrm{tr}\left(\mathbf{F}\left(\mathbf{D}^{\frac{1}{2}}\mathbf{H}\mathbf{Q}\mathbf{H}^H\mathbf{D}^{\frac{1}{2}} + \sigma_r^2\mathbf{I}_{N_r}\right)\mathbf{F}^H\right) \le E_m \tag{13c}$$

$$\mathrm{tr}\left(\mathbf{F}\left(\mathbf{D}^{\frac{1}{2}}\mathbf{H}\mathbf{Q}\mathbf{H}^H\mathbf{D}^{\frac{1}{2}} + \sigma_r^2\mathbf{I}_{N_r}\right)\mathbf{F}^H\right) + N_r P_c \le \eta\,\mathrm{tr}\left(\left(\mathbf{I}_{N_r} - \mathbf{D}\right)\mathbf{H}\mathbf{Q}\mathbf{H}^H\right) \tag{13d}$$

$$\mathbf{Q} \ge 0, \quad 0 \le d_i \le 1, \quad i = 1,\ldots,N_r \tag{13e}$$

where $E_m = (1-\xi)E'_m - N_r P_c$, $\eta = \eta_1(1-\xi)$, and $P$ is the power available at the source node. Note that (13c) and (13d) are the sum energy constraint across all data streams, while in [23], an energy constraint is imposed on each data stream. Thus, the problem in (13) has a larger feasible region than the problem in [23]. Hence, the transceivers designed under problem (13) should have a better performance than those in [23]. This will be shown further in next sections.

## III. Proposed Transceiver Optimization Algorithms

The transceiver design problem (13) is nonconvex with matrix variables. In particular, the complicated objective function in (13a) and the constraint in (13d) make problem (13) difficult to solve. In this section, we first derive the structure of $\mathbf{Q}$, $\mathbf{D}$, and $\mathbf{F}$, with which the problem (13) can be reduced to a simpler joint source and relay power allocation problem with scalar variables. Then we propose three algorithms to efficiently solve the power allocation problem which achieve various performance-complexity trade-offs.

Based on Hadamard's inequality on matrix determinant, the objective function (13a) is maximized if $\mathbf{D}^{\frac{1}{2}}\mathbf{H}\mathbf{Q}\mathbf{H}^H\mathbf{D}^{\frac{1}{2}}\mathbf{F}^H\mathbf{G}^H(\sigma_r^2\mathbf{G}\mathbf{F}\mathbf{F}^H\mathbf{G}^H + \sigma_d^2\mathbf{I}_{N_d})^{-1}\mathbf{G}\mathbf{F}$ is a diagonal matrix. Towards this end and considering that $\mathbf{D}$ is diagonal, we design $\mathbf{Q}$ and $\mathbf{D}$ such that

$$\mathbf{D}^{\frac{1}{2}}\mathbf{H}\mathbf{Q}\mathbf{H}^H\mathbf{D}^{\frac{1}{2}} = \mathbf{\Sigma} \tag{14}$$

where $\mathbf{\Sigma}$ is an $N_r \times N_r$ diagonal matrix. Based on (14), it can be seen that the problem of optimizing $\mathbf{F}$ is given by

$$\max_{\mathbf{F}} \quad \log\left|\mathbf{I}_{N_d} + \mathbf{G}\mathbf{F}\mathbf{\Sigma}\mathbf{F}^H\mathbf{G}^H(\sigma_r^2\mathbf{G}\mathbf{F}\mathbf{F}^H\mathbf{G}^H + \sigma_d^2\mathbf{I}_{N_d})^{-1}\right| \tag{15a}$$

$$\text{s.t.} \quad \mathrm{tr}\left(\mathbf{F}(\mathbf{\Sigma} + \sigma_r^2\mathbf{I}_{N_r})\mathbf{F}^H\right) \le E_m \tag{15b}$$

$$\mathrm{tr}\left(\mathbf{F}(\mathbf{\Sigma} + \sigma_r^2\mathbf{I}_{N_r})\mathbf{F}^H\right) + N_r P_c \le \eta\,\mathrm{tr}\left(\left(\mathbf{I}_{N_r} - \mathbf{D}\right)\mathbf{H}\mathbf{Q}\mathbf{H}^H\right) \tag{15c}$$

where we omit the constant $1/2$ in the objective function (15a).

Let us denote

$$\mathbf{G} = \mathbf{U}_g\mathbf{\Lambda}_g^{\frac{1}{2}}\mathbf{V}_g^H \tag{16}$$

as the singular value decomposition (SVD) of $\mathbf{G}$, where the dimension of $\mathbf{\Lambda}_g$ is $N_d \times N_r$ and its diagonal elements are sorted in decreasing order. It can be proven using the results in [12] that the optimal $\mathbf{F}$ as the solution to the problem in (15) is

$$\mathbf{F} = \mathbf{V}_g\mathbf{\Lambda}_f^{\frac{1}{2}} \tag{17}$$

where $\mathbf{\Lambda}_f$ is an $N_r \times N_r$ diagonal matrix. Considering that the largest number of concurrent data streams for information transmission supported by this relay system is $K = \min(N_s, N_r, N_d)$, the optimal $\mathbf{\Lambda}_f$ satisfies $\mathbf{\Lambda}_f = \mathrm{bd}(\mathbf{\Lambda}_{f,1}, \mathbf{0}_{N_r-K})$, where $\mathrm{bd}(\cdot)$ denotes a block diagonal matrix, $\mathbf{\Lambda}_{f,1}$ is a $K \times K$ diagonal matrix, and $\mathbf{0}_n$ stands for an $n \times n$ matrix with all zero elements.

Similarly, considering the maximal number of concurrent data streams is $K$, based on (14) we choose $\mathbf{D}$ as

$$\mathbf{D} = \mathrm{bd}(\mathbf{D}_1, \mathbf{0}_{N_r-K}) \tag{18}$$

where $\mathbf{D}_1$ is a $K \times K$ diagonal matrix. This implies that signals at $K$ antennas of the relay node are used for both EH and information transmission, while the remaining $N_r - K$ relay antennas are used solely for EH (i.e., $d_i = 0, i = K+1,\ldots,N_r$). Thus, (14) is achievable by

$$\mathbf{H}_1\mathbf{Q}\mathbf{H}_1^H = \mathbf{\Lambda} \tag{19}$$

where $\mathbf{\Lambda}$ is a $K \times K$ diagonal matrix, and $\mathbf{H}_1$ contains the first $K$ rows of $\mathbf{H}$. Let us introduce

$$\mathbf{H}_1 = \mathbf{U}_h\mathbf{\Lambda}_h^{\frac{1}{2}}\mathbf{V}_h^H \tag{20}$$

as the SVD of $\mathbf{H}_1$, where $\mathbf{\Lambda}_h$ is a $K \times K$ diagonal matrix. From (19) and (20), we have

$$\mathbf{Q} = \mathbf{V}_h\mathbf{\Lambda}_h^{-\frac{1}{2}}\mathbf{U}_h^H\mathbf{\Lambda}\mathbf{U}_h\mathbf{\Lambda}_h^{-\frac{1}{2}}\mathbf{V}_h^H. \tag{21}$$

From (17), (18), and (21), the transceiver optimization problem in (13) can be rewritten as

$$\max_{\mathbf{\Lambda},\mathbf{\Lambda}_{f,1},\mathbf{D}_1} \quad \log\left|\mathbf{I}_K + \mathbf{\Lambda}_{g,1}\mathbf{\Lambda}_{f,1}\mathbf{D}_1\mathbf{\Lambda} \times (\sigma_r^2\mathbf{\Lambda}_{g,1}\mathbf{\Lambda}_{f,1} + \sigma_d^2\mathbf{I}_K)^{-1}\right| \tag{22a}$$

$$\text{s.t.} \quad \mathrm{tr}(\mathbf{\Lambda}\mathbf{U}_h\mathbf{\Lambda}_h^{-1}\mathbf{U}_h^H) \le P \tag{22b}$$

[3]With the diode current analysis based nonlinear EH model [40] it has been shown in [40], [41], [48], [49] that input signal properties including the waveform, modulation, and distribution have impact on the system design. For instance, as explained in [40] that considering the rectifier nonlinearity, a nonzero mean Gaussian input distribution outperforms the conventional zero-mean Gaussian input distribution in multicarrier transmissions in terms of the harvested energy. In this paper, we assume that the input signal has zero-mean Gaussian distribution. Consequently, we only consider the optimization of the covariance matrix $\mathbf{Q}$ at the source node. Although such Gaussian signalling makes the optimization problem tractable, it is suboptimal.

$$\mathrm{tr}(\mathbf{\Lambda}_{f,1}(\mathbf{D}_1\mathbf{\Lambda}+\sigma_r^2\mathbf{I}_{N_r}))\le E_m \tag{22c}$$

$$\mathrm{tr}(\mathbf{\Lambda}_{f,1}(\mathbf{D}_1\mathbf{\Lambda}+\sigma_r^2\mathbf{I}_{N_r}))\le \eta\,\mathrm{tr}((\mathbf{I}_K-\mathbf{D}_1)\mathbf{\Lambda}) + \eta\,\mathrm{tr}(\tilde{\mathbf{H}}\mathbf{\Lambda}\tilde{\mathbf{H}}^H)-N_rP_c \tag{22d}$$

$$0\le d_i\le 1,\ \tilde{\lambda}_{f,i}\ge 0,\ \tilde{\lambda}_i\ge 0,\ i=1,\ldots,K \tag{22e}$$

where the constant $1/2$ in (13a) is omitted in (22a), $\mathbf{\Lambda}_{g,1}$ contains the largest $K$ singular values of $\mathbf{G}$, $\tilde{\mathbf{H}}=\mathbf{H}_2\mathbf{V}_h\mathbf{\Lambda}_h^{-\frac{1}{2}}\mathbf{U}_h^H$, $\mathbf{H}_2$ contains the last $N_r-K$ rows of $\mathbf{H}$, $\tilde{\lambda}_{f,i}$ and $\tilde{\lambda}_i$ are the $i$th main diagonal element of $\mathbf{\Lambda}_f$ and $\mathbf{\Lambda}$, respectively. As $\mathbf{\Lambda}$, $\mathbf{\Lambda}_{f,1}$, $\mathbf{D}_1$, and $\mathbf{\Lambda}_{g,1}$ are diagonal matrices, the problem in (22) can be equivalently rewritten to the following problem with scalar optimization variables

$$\max_{\mathbf{d},\boldsymbol{\lambda},\boldsymbol{\lambda}_f}\ \sum_{i=1}^{K}\log\left(1+\frac{d_i\lambda_i\lambda_{f,i}\lambda_{g,i}}{1+\lambda_{f,i}\lambda_{g,i}}\right) \tag{23a}$$

$$\text{s.t.}\quad \sum_{i=1}^{K}a_i\lambda_i\le\sigma_r^{-2}P \tag{23b}$$

$$\sum_{i=1}^{K}\lambda_{f,i}(d_i\lambda_i+1)\le E_m \tag{23c}$$

$$\sum_{i=1}^{K}\lambda_{f,i}(d_i\lambda_i+1)\le\eta\sigma_r^2\sum_{i=1}^{K}(c_i-d_i)\lambda_i-N_rP_c \tag{23d}$$

$$0\le d_i\le 1,\ \lambda_{f,i}\ge 0,\ \lambda_i\ge 0,\ i=1,\ldots,K \tag{23e}$$

where $a_i$ and $c_i$ are the $i$th diagonal element of $\mathbf{U}_h\mathbf{\Lambda}_h^{-1}\mathbf{U}_h^H$ and $\mathbf{I}_K+\tilde{\mathbf{H}}^H\tilde{\mathbf{H}}$, respectively, $\lambda_i=\tilde{\lambda}_i/\sigma_r^2$, $\lambda_{g,i}=\tilde{\lambda}_{g,i}/\sigma_d^2$, $\lambda_{f,i}=\tilde{\lambda}_{f,i}\sigma_r^2$, $\tilde{\lambda}_{g,i}$ is the $i$th main diagonal element of $\mathbf{\Lambda}_g$, $\mathbf{d}=[d_1,\ldots,d_K]^T$, $\boldsymbol{\lambda}=[\lambda_1,\ldots,\lambda_K]^T$, $\boldsymbol{\lambda}_f=[\lambda_{f,1},\ldots,\lambda_{f,K}]^T$, and $(\cdot)^T$ denotes the matrix transpose.

By introducing $x_i=\lambda_i$, $b_i=\lambda_{g,i}$, $y_i=\lambda_{f,i}(d_i\lambda_i+1)$, $i=1,\ldots,K$, the problem in (23) can be rewritten as

$$\max_{\mathbf{d},\mathbf{x},\mathbf{y}}\ \sum_{i=1}^{K}\log\left(1+\frac{d_ix_ib_iy_i}{1+d_ix_i+b_iy_i}\right) \tag{24a}$$

$$\text{s.t.}\quad \sum_{i=1}^{K}a_ix_i\le\sigma_r^{-2}P \tag{24b}$$

$$\sum_{i=1}^{K}y_i\le E_m \tag{24c}$$

$$\sum_{i=1}^{K}y_i\le\eta\sigma_r^2\sum_{i=1}^{K}(c_i-d_i)x_i-N_rP_c \tag{24d}$$

$$0\le d_i\le 1,\ x_i\ge 0,\ y_i\ge 0,\quad i=1,\ldots,K \tag{24e}$$

where $\mathbf{x}=[x_1,\ldots,x_K]^T$ and $\mathbf{y}=[y_1,\ldots,y_K]^T$. Let us introduce $w_i=d_ix_i$, $i=1,\ldots,K$. Then the problem in (24) can be recast as

$$\max_{\mathbf{w},\mathbf{x},\mathbf{y}}\ \sum_{i=1}^{K}\log\left(1+\frac{w_ib_iy_i}{1+w_i+b_iy_i}\right) \tag{25a}$$

$$\text{s.t.}\quad \sum_{i=1}^{K}a_ix_i\le\sigma_r^{-2}P \tag{25b}$$

$$\sum_{i=1}^{K}y_i\le E_m \tag{25c}$$

$$\sum_{i=1}^{K}y_i\le\eta\sigma_r^2\sum_{i=1}^{K}(c_ix_i-w_i)-N_rP_c \tag{25d}$$

$$x_i\ge w_i\ge 0,\ \ y_i\ge 0,\quad i=1,\ldots,K \tag{25e}$$

where $\mathbf{w}=[w_1,\ldots,w_K]^T$. The original variables $d_i$, $\lambda_i$, and $\lambda_{f,i}$, $i=1,\ldots,K$, can be recovered from the solution of the problem (25) as

$$d_i=\begin{cases}w_i/x_i & x_i\ne 0\\ 0 & x_i=0\end{cases},\ \ \lambda_i=x_i,\ \ \lambda_{f,i}=y_i/(w_i+1).$$

In the following subsections, we develop three methods to efficiently solve the optimal power allocation problem in (25), which provide various performance-complexity trade-offs.

### *A. Proposed Method 1*

By introducing $\frac{w_ib_iy_i}{1+w_i+b_iy_i}\ge t_i, i=1,\ldots,K$, the problem in (25) can be equivalently written as the following problem

$$\max_{\mathbf{w},\mathbf{x},\mathbf{y},\mathbf{t}}\ \sum_{i=1}^{K}\log(1+t_i) \tag{26a}$$

$$\text{s.t.}\quad \frac{w_ib_iy_i}{1+w_i+b_iy_i}\ge t_i,\quad i=1,\ldots,K \tag{26b}$$

$$\sum_{i=1}^{K}a_ix_i\le\sigma_r^{-2}P \tag{26c}$$

$$\sum_{i=1}^{K}y_i\le E_m \tag{26d}$$

$$\sum_{i=1}^{K}y_i\le\eta\sigma_r^2\sum_{i=1}^{K}(c_ix_i-w_i)-N_rP_c \tag{26e}$$

$$x_i\ge w_i\ge 0,\ \ y_i\ge 0,\quad i=1,\ldots,K \tag{26f}$$

where $\mathbf{t}=[t_1,\ldots,t_K]^T$. Although $\log(1+t_i)$ is a concave function of $t_i$, constraints in (26b) cannot be proven to be convex. Therefore, the problem in (26) is a nonconvex problem. In this paper, we apply the sequential quadratic programming (SQP) [35] method to solve the problem in (26). SQP is an iterative algorithm where each search direction is obtained by solving a particular quadratic programming (QP) subproblem, which is obtained by a quadratic model of the objective function (26a) and a linearization of the constraints in (26b). Different from the second-order Taylor series approximation of the objective function (26a), the second-order term in the quadratic model is

a positive definite approximation of the Hessian matrix of the Lagrangian function of the problem (26), so that the curvature of the constraints (26b)–(26f) is also taken into consideration. After the search direction is obtained, the optimization variables, the Lagrange multipliers, and the approximation of the Hessian matrix of the Lagrangian function are updated by the gradient method in each iteration until the optimization variables and the Lagrange multipliers converge to a local optimum. More details of the SQP method can be found in [35]. The computational complexity order of solving each QP subproblem by the primal-dual potential reduction method is $\mathcal{O}((4K)^{4.5})$. The overall complexity of the SQP approach depends on the number of iterations, which may depend on the given batch of data. Considering that the complexity order of calculating the SVDs of $\mathbf{H}_1$ in (20) and $\mathbf{G}$ in (16) is $\mathcal{O}(K^3 + N_s^2 K)$ and $\mathcal{O}(N_d^3 + N_r^2 N_d)$, respectively, the total computational complexity order of solving the problem in (13) through method 1 is $\mathcal{O}(K^3 + N_s^2 K + N_d^3 + N_r^2 N_d + c_1(4K)^{4.5})$, where $c_1$ is the number of iterations in the SQP approach.

### B. Proposed Method 2

This method converts the problem in (25) to a convex problem by exploiting the following upper bound

$$\frac{w_i b_i y_i}{1 + w_i + b_i y_i} \leq \frac{w_i b_i y_i}{w_i + b_i y_i}. \tag{27}$$

Using (27), the problem in (25) can be rewritten as

$$\max_{\mathbf{w},\mathbf{x},\mathbf{y},\mathbf{t}} \left(\prod_{i=1}^{K} t_i\right)^{\frac{1}{K}} \tag{28a}$$

$$\text{s.t.} \quad 1 + \frac{w_i b_i y_i}{w_i + b_i y_i} \geq t_i, \quad i = 1, \ldots, K \tag{28b}$$

$$\sum_{i=1}^{K} a_i x_i \leq \sigma_r^{-2} P \tag{28c}$$

$$\sum_{i=1}^{K} y_i \leq E_m \tag{28d}$$

$$\sum_{i=1}^{K} y_i \leq \eta \sigma_r^2 \sum_{i=1}^{K} (c_i x_i - w_i) - N_r P_c \tag{28e}$$

$$x_i \geq w_i \geq 0, \quad y_i \geq 0, \quad i = 1, \ldots, K. \tag{28f}$$

Now we show constraints in (28b) can be converted to semidefinite constraints. From (28b) we have

$$\begin{aligned} &\frac{w_i b_i y_i}{w_i + b_i y_i} - t_i - 1 \\ &\quad = \frac{(w_i + b_i y_i)^2 - w_i^2 - b_i^2 y_i^2}{2(w_i + b_i y_i)} - t_i - 1 \geq 0. \end{aligned} \tag{29}$$

Inequality (29) is equivalent to

$$\begin{aligned} &w_i + b_i y_i - w_i (w_i + b_i y_i)^{-1} w_i \\ &\quad - b_i y_i (w_i + b_i y_i)^{-1} b_i y_i - 2t_i - 2 \geq 0 \end{aligned}$$

which can be rewritten as the following semidefinite constraint

$$\begin{pmatrix} w_i + b_i y_i - 2t_i - 2 & w_i & b_i y_i \\ w_i & w_i + b_i y_i & 0 \\ b_i y_i & 0 & w_i + b_i y_i \end{pmatrix} \geq 0. \tag{30}$$

By substituting (28b) with (30), we obtain the following optimization problem

$$\max_{\mathbf{w},\mathbf{x},\mathbf{y},\mathbf{t}} \left(\prod_{i=1}^{K} t_i\right)^{\frac{1}{K}} \tag{31a}$$

$$\text{s.t.} \quad \begin{pmatrix} w_i + b_i y_i - 2t_i - 2 & w_i & b_i y_i \\ w_i & w_i + b_i y_i & 0 \\ b_i y_i & 0 & w_i + b_i y_i \end{pmatrix} \geq 0$$

$$i = 1, \ldots, K \tag{31b}$$

$$\sum_{i=1}^{K} a_i x_i \leq \sigma_r^{-2} P \tag{31c}$$

$$\sum_{i=1}^{K} y_i \leq E_m \tag{31d}$$

$$\sum_{i=1}^{K} y_i \leq \eta \sigma_r^2 \sum_{i=1}^{K} (c_i x_i - w_i) - N_r P_c \tag{31e}$$

$$x_i \geq w_i \geq 0, \quad y_i \geq 0, \quad i = 1, \ldots, K. \tag{31f}$$

The problem in (31) is convex as the objective function (31a) is a geometric mean which is a concave function [52], (31b) is a positive semidefinite constraint and (31b)–(31f) are linear constraints. This problem can be solved efficiently using the disciplined convex programming toolbox CVX [36]. As (31a) is a nonlinear function, the problem in (31) is a nonlinear SDP problem. The computational complexity of solving this class of problems is an active research area [53]. It can be shown using the results in [53] that by using the augmented Lagrangian method, the problem in (31) can be solved at a complexity of $\mathcal{O}(c_2 K(6K + 2)^3)$, where $c_2$ denotes the number of iterations required till convergence. Therefore, considering the complexity of calculating the SVDs of $\mathbf{H}_1$ and $\mathbf{G}$, the overall computational complexity order of solving the problem in (13) by method 2 is $\mathcal{O}(K^3 + N_s^2 K + N_d^3 + N_r^2 N_d + c_2 K(6K + 2)^3)$. Thus, the complexity of the proposed method 2 is lower than that of the proposed method 1.

### C. Proposed Method 3

This method exploits the following lower bound

$$\begin{aligned} 1 + \frac{w_i b_i y_i}{1 + w_i + b_i y_i} &= \frac{(1 + w_i)(1 + b_i y_i)}{1 + w_i + b_i y_i} \\ &\geq \frac{(1 + w_i)(1 + b_i y_i)}{2 + w_i + b_i y_i}. \end{aligned} \tag{32}$$

Using (32), the problem in (25) can be written as

$$\min_{\mathbf{w},\mathbf{x},\mathbf{y}} \sum_{i=1}^{K} \log\left(\frac{1}{1+w_i}+\frac{1}{1+b_i y_i}\right) \tag{33a}$$

$$\text{s.t.} \quad \sum_{i=1}^{K} a_i x_i \le \sigma_r^{-2} P \tag{33b}$$

$$\sum_{i=1}^{K} y_i \le E_m \tag{33c}$$

$$\sum_{i=1}^{K} y_i \le \eta\sigma_r^2 \sum_{i=1}^{K}(c_i x_i - w_i) - N_r P_c \tag{33d}$$

$$x_i \ge w_i \ge 0,\ y_i \ge 0, \quad i = 1,\ldots,K. \tag{33e}$$

It can be shown through its Hessian matrix that the objective function in (33a) is a convex function. Therefore, the problem in (33) is a convex optimization problem. We develop a primal-dual based interior-point method to solve the problem in (33) according to the steps in Algorithm 11.2 of [52]. It can be shown that the major computation in each primal-dual search of the proposed method 3 is the calculation of the inverse of a $(6K+2)\times(6K+2)$ matrix. Thus, the per iteration computational complexity order of the proposed method 3 is $\mathcal{O}((6K+2)^3)$. Considering the complexity of calculating the SVDs of $\mathbf{H}_1$ and $\mathbf{G}$, the overall complexity of solving the problem in (13) using the method 3 is $\mathcal{O}(K^3+N_s^2K+N_d^3+N_r^2N_d+c_3(6K+2)^3)$, where $c_3$ is the number of iterations till convergence. It can be seen that the complexity of the proposed method 3 is lower than the proposed method 1 and method 2. The theoretical analysis of the gap between the three proposed methods is difficult as it strongly depends on random channel realizations. It will be shown in Section IV that the system MI gaps between the method 1 and the other two methods are very small.

For the uniform PS algorithm in [29], since two loops of iterations are required to optimize the source and relay precoding matrices, its computational complexity can be estimated as $\mathcal{O}(N_r^3+N_s^2N_r+N_d^3+N_r^2N_d+c_4(c_5+c_6)K)$, where $c_4$ is the number of outer iterations, $c_5$ and $c_6$ are the number of inner iterations for optimizing the source precoding and the relay precoding, respectively. We would like to note that as very small step sizes ($10^{-3}$ and $10^{-4}$) are used in the inner iterations [29], $c_5$ and $c_6$ can be very large.

## IV. Numerical Examples

We investigate the performance of the three proposed transceiver design algorithms through numerical simulations in this section. We consider a relay system where the source node, the relay node, and the destination node are placed in one line as illustrated in Fig. 2. This simulation setup is chosen to facilitate the investigation of the system performance with respect to the relay position. The distance from the source to the destination is $D_{sd}=20$ meters, while the source-relay distance is $D_{sr}=10L$ meters, and the relay-destination distance is $D_{rd}=10(2-L)$ meters. Here we normalize $L$ $(0<L<2)$ over a distance of 10 meters. This normalization enables an easy identification of whether the relay node is placed nearby the destination node $(1<L<2)$ or closer to the source node $(0<L<1)$. In the simulations,[4] we set $0.25<L<1.75$ such that $D_{sr}>2.5$ and $D_{rd}>2.5$.

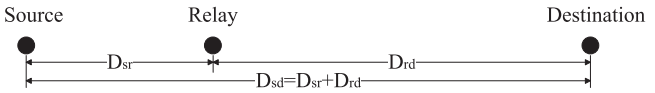


Fig. 2. Locations of the source, relay, and destination nodes.

Following [27], [28], and [56], we set the channel matrices as $\mathbf{H}=D_{sr}^{-\zeta/2}\bar{\mathbf{H}}$ and $\mathbf{G}=D_{rd}^{-\zeta/2}\bar{\mathbf{G}}$, where $D_{sr}^{-\zeta}$ and $D_{rd}^{-\zeta}$ denote the large-scale path loss, while $\bar{\mathbf{H}}$ and $\bar{\mathbf{G}}$ are the small-scale channel fading with Rayleigh distribution. In this paper, we consider the suburban environment with the path loss exponent $\zeta=3$ [56]. Matrices $\bar{\mathbf{H}}$ and $\bar{\mathbf{G}}$ have independent and identically distributed (i.i.d.) complex Gaussian entries with zero-mean and variances of $1/N_s$ and $1/N_r$, respectively. The noise variances at the relay and destination nodes are set as $\sigma_r^2=\sigma_d^2=-50$ dBm. For all numerical examples, we set $\eta=0.8$ and $P_c=1$ $\mu$W. The performances of the three proposed methods are compared with

1) A benchmark WPC relay system where the problem (26) is solved without the peak EH constraint (26d).
2) The per data stream energy constraint based algorithm in [23].
3) The TS based AF MIMO relay system in [30] with peak transmission power constraints, where the limits of the source node peak transmission power $P_{m,s}$ and the relay node peak power $P_{m,r}$ are set to $P_{m,s}=P_{m,r}=2P$.
4) The uniform PS-based joint source and relay design algorithm in [29].

Note that these four algorithms are based on linear EH models. All numerical simulation results are obtained by averaging over 1000 independent realizations of $\bar{\mathbf{H}}$ and $\bar{\mathbf{G}}$.

### A. Example 1: System MI Versus the Source Node Power

In our first numerical simulation example, we choose a relay location with $L=1$. The system MI achieved by the proposed method 1 with $N_r=1$, $N_s=N_d=3$, and various peak power constraint $E_m$ is shown in Fig. 3 versus the source node power $P$. It can be seen that with a linear EH model in the benchmark relay system, the system MI increases linearly with $P$ (in dBm). However, this linear EH model does not fit practical EH circuits. Using the practical nonlinear EH model (7), as the energy available at the relay node for signal transmission is limited by $E_m$, the system MI curve bends down when $P$ increases and eventually remains flat at large $P$. Moreover, Fig. 3 shows that at high $P$, the achievable MI of the three proposed algorithms decreases when $E_m$ decreases.

The system MI achieved by the seven algorithms tested at various source node power $P$ is illustrated in Fig. 4 for

[4] As reported in [54] for commercial products and Table 1 of [55], such source-relay distance is among typical practical distances of RF-based wireless power transfer. Considering RF signals at the 915 MHz band [39], this distance is in the far-filed of the antenna pattern.

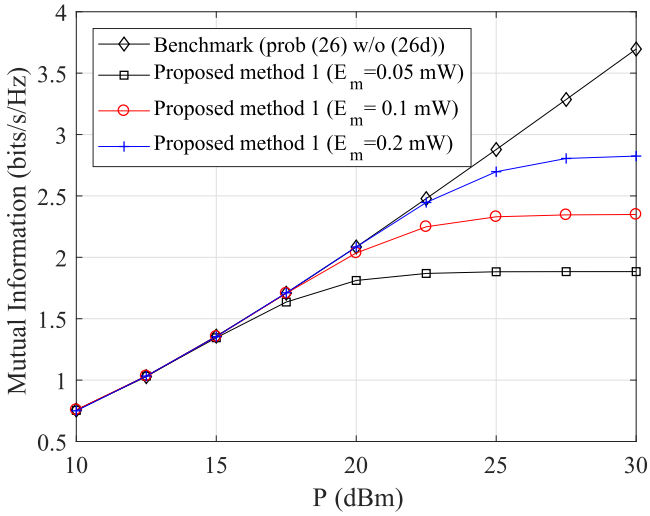


Fig. 3. Example 1: MI of the proposed method 1 versus $P$ at various $E_m$; $L = 1$, $N_r = 1$, and $N_s = N_d = 3$.

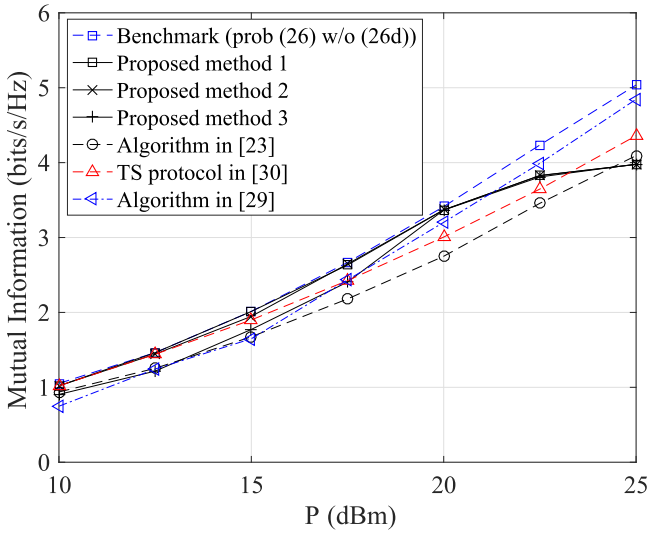


Fig. 4. Example 1: MI versus $P$; $L = 1$, $E_m = 0.2$ mW, and $N_s = N_r = N_d = 3$.

$E_m = 0.2$ mW and $N_s = N_r = N_d = 3$. We can see from Fig. 4 that among the four linear EH based systems, the benchmark algorithm has a larger system MI than the per data stream energy constraints based algorithm in [23], the TS protocol in [30], and the uniform PS approach in [29]. In particular, the MI gap between the benchmark algorithm and that of the algorithms in [23] and [30] increases with $P$. The gain of the benchmark algorithm over [23] is mainly contributed by the sum energy constraint (12) across all data streams, compared with the per data stream energy constraint. The MI gain of the benchmark algorithm over [29] is achieved by different PS ratios across data streams. The gain of the benchmark algorithm over the TS protocol in [30] can be explained below. In the TS protocol, all sub-channels use the same TS factor to adjust the time duration for the energy transfer and the information transmission. Using

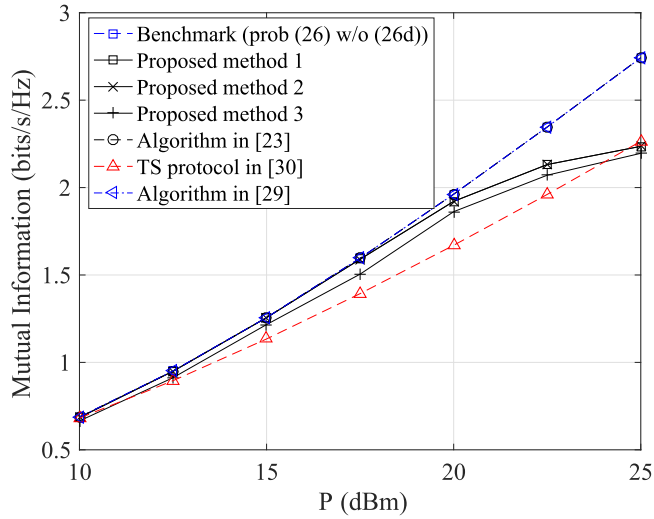


Fig. 5. Example 1: MI versus $P$; $L = 1$, $E_m = 0.1$ mW, $N_r = 1$, and $N_s = N_d = 3$.

the benchmark algorithm, the PS ratio in each sub-channel for the information and energy transmission can be different. Thus, it provides more flexibility in the system resource allocation, which yields a higher source-destination MI.[5] As the benchmark algorithm achieves a higher data rate and consumes the same amount of transmission power at the source node as the algorithms in [23], [29], and [30], the proposed scheme has a higher power efficiency in terms of the achieved data rate per unit power of the source node.

It can be seen from Fig. 4 that at low and medium $P$, the proposed method 1 and method 2 have the same MI as the benchmark system, and a higher MI than the other three linear EH based systems. Due to the limit of $E_m$, the achievable MI of the three proposed algorithms decreases at high $P$.

Fig. 5 illustrates the system MI achieved by the seven algorithms tested with respect to the source node power $P$ with $E_m = 0.1$ mW, $N_r = 1$, and $N_s = N_d = 3$. It can be observed from Fig. 5 that when $N_r = 1$, the algorithms in [23] and [29] have the same MI as the benchmark system. The reason is that the uniform PS scheme becomes optimal where there is only a single antenna at the relay node. Moreover, with $N_r = 1$, the number of concurrent data streams is $K = 1$, and thus, the algorithm in [23] also becomes optimal. Figs. 4 and 5 clearly indicate that using the same PS ratio across all relay antennas [29] or the per data stream energy constraint [23] is suboptimal for $K > 1$ and/or $N_r > 1$. It can also be seen from Fig. 5 that the PS based WPC relay systems have a higher MI than the TS based system in [30], due to the peak source node power constraint in [30].

Similar to Fig. 4, it can be seen from Fig. 5 that due to the limit of $E_m$, at high $P$, the three proposed methods have a lower MI than the three linear EH based PS systems. Interestingly, it can be seen from Figs. 4 and 5 that the system MI yielded by

[5]Note that the performance benefits of PS versus TS also depends on the EH model and the signal design. As explained in [40] with a diode current analysis based nonlinear EH model, sometimes TS is preferred over PS, and a combination of PS and TS is in general the best strategy.

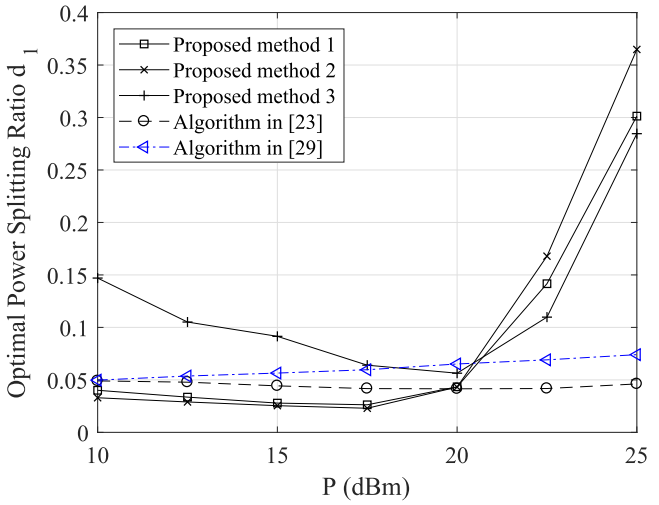


Fig. 6. Example 2: The optimal $d_1$ versus $P$; $N_s = N_r = N_d = 3$, $L = 1$, and $E_m = 0.2$ mW.

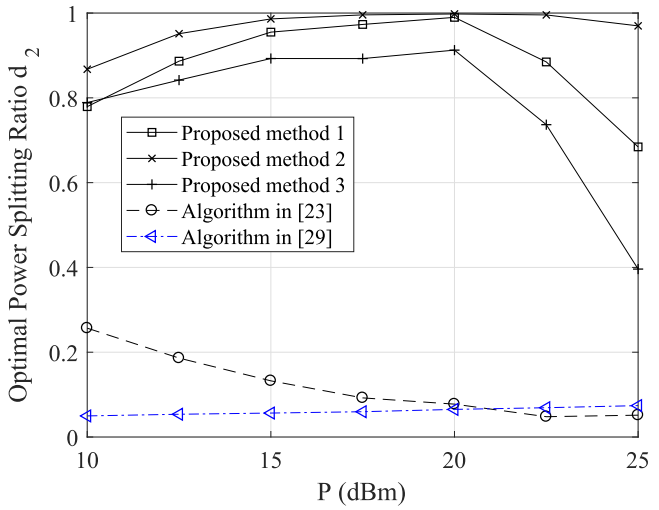


Fig. 7. Example 2: The optimal $d_2$ versus $P$; $N_s = N_r = N_d = 3$, $L = 1$, and $E_m = 0.2$ mW.

the three proposed methods is very close to each other at large $P$. The reason is given below. For the upper bound and lower bound based methods, the bounding errors in (27) and (32) are very small as $w_i$ and $b_i y_i$ are much bigger than 1 in real wireless WPC environments. Thus, the three proposed methods converge to the same performance as $P$ increases. At low to medium $P$, the proposed method 3 has a slightly lower MI than that of the proposed method 1 and method 2. Considering that the former algorithm has a lower computational complexity, it is attractive for practical wireless powered AF MIMO relay systems. From Fig. 4 and Fig. 5, we can observe that the system MI increases when the number of antennas at the relay node increases, which reflects the benefit of MIMO systems.

### *B. Example 2: Power Splitting Ratios at Various Source Node Transmission Power*

In our second numerical example, we choose $N_s = N_r = N_d = 3$, $E_m = 0.2$ mW, and $L = 1$. The PS ratios $d_1$, $d_2$, and $d_3$ computed as optimal by the three proposed algorithms, the algorithm in [23], and the approach in [29] at various source power $P$ are illustrated in Figs. 6, 7, and 8, respectively. The optimal $d_1$, $d_2$, and $d_3$ of the proposed method 1 versus $P$ is illustrated in Fig. 9. It can be observed from Figs. 6–8 that for each $d_i$ the optimal PS ratio from the three proposed methods follows a similar trend. In particular, the optimal PS ratios of the proposed method 1 and method 2 are very close to each other, which explains the observation in Fig. 4 that these two methods yield a very similar MI. We can also observe from Figs. 6–8 that the algorithm in [23] yields a quite different $d_i$ compared with the three proposed methods.

Interestingly, we can observe that compared with the algorithm in [23], the three proposed methods have a larger variation of the PS ratios throughout the range of $P$. This indicates that to maximize the system MI, it is important to consider a general energy constraint in (12), instead of per data stream energy constraints. It can also be observed from Figs. 6–9 that $d_1$, $d_2$, and $d_3$ follow different trends versus $P$. This justifies the importance of choosing different PS ratios across data streams compared with the uniform PS approach in [29].

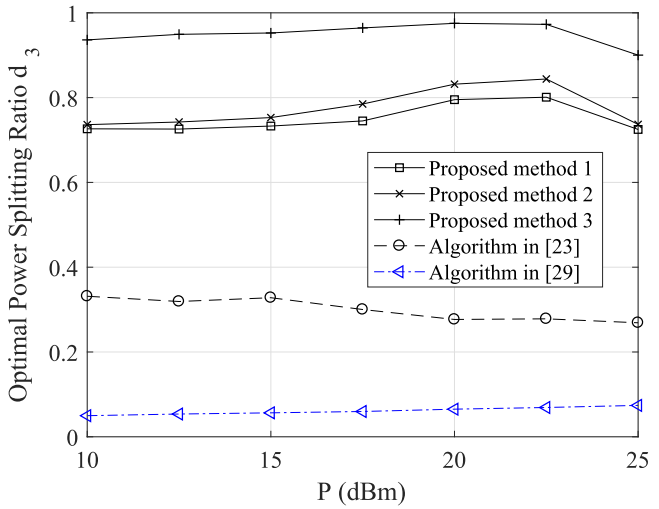


Fig. 8. Example 2: The optimal $d_3$ versus $P$; $N_s = N_r = N_d = 3$, $L = 1$, and $E_m = 0.2$ mW.

### *C. Example 3: Achievable Source-Destination MI at Various Positions of the Relay Node*

In the last numerical simulation example, we study the system MI at different source-relay distances. We choose $N_s = N_r = N_d = 3$, $E_m = 0.2$ mW, and investigate the achievable system MI at different $L$. Fig. 10 illustrates the system MI of the proposed method 1, the algorithm in [23], and the approach in [29] versus $P$ at different $L$. The performance of the other two proposed methods is not demonstrated in Fig. 10 as they have a similar system MI as the proposed method 1. It can be seen that for $L = 1.6$, the achievable MI of the proposed method 1 is higher than the algorithms in [23] and [29]. For $L = 1.2$,

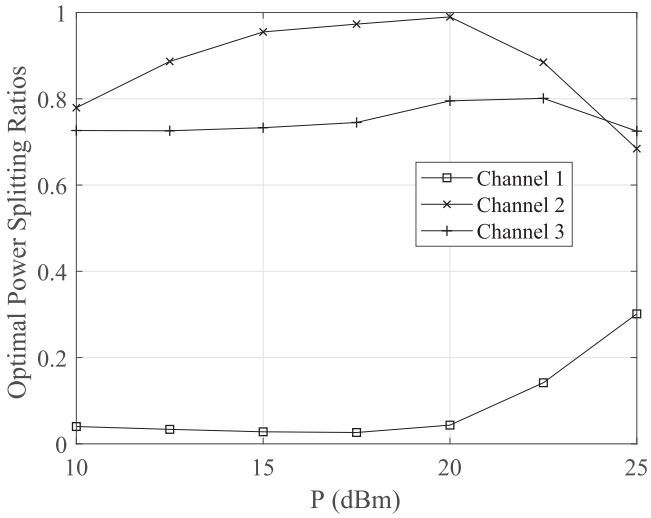


Fig. 9. Example 2: The optimal $d_1$, $d_2$, and $d_3$ of the proposed method 1 versus $P$; $N_s = N_r = N_d = 3$, $L = 1$, and $E_m = 0.2$ mW.

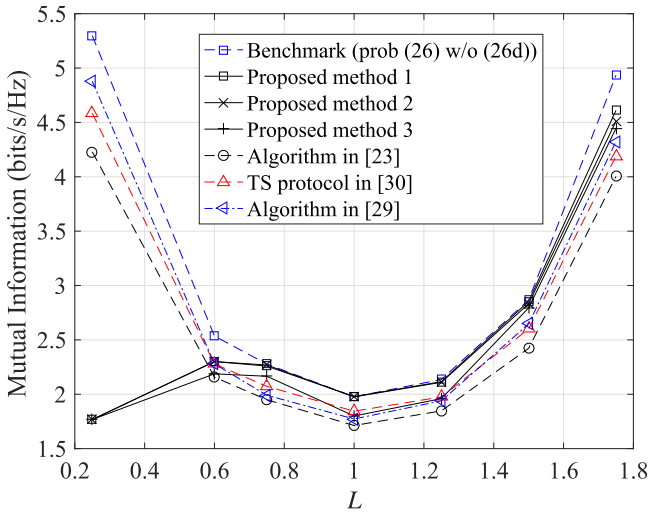


Fig. 11. Example 3: MI versus $L$; $P = 15$ dBm, $E_m = 0.2$ mW, and $N_s = N_r = N_d = 3$.

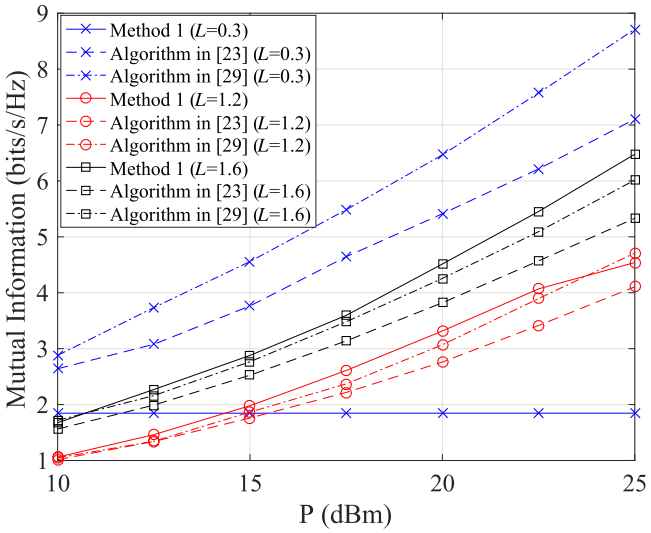


Fig. 10. Example 3: MI of the proposed method 1 versus $P$ at various $L$; $N_s = N_r = N_d = 3$ and $E_m = 0.2$ mW.

the proposed method 1 has a higher MI than the other two algorithms except for $P = 25$ dBm. At $L = 0.3$, the proposed method 1 yields a lower system MI. The reason is that for the practical nonlinear EH model (7), at $L = 0.3$, the energy harvested by the relay node is limited by $E'_m$, not $P$. As a result, the increase of $P$ does not lead to an increase of the system MI. This explanation also applies to the performance of the proposed method 1 at $L = 1.2$ and $P = 25$ dBm. Interestingly, we find that the constraint (26d) is inactive at $L = 1.6$ for the range of $P$ tested.

Fig. 11 illustrates the system MI of the seven algorithms tested versus $L$ with $E_m = 0.2$ mW, $N_s = N_r = N_d = 3$, and $P = 15$ dBm. We can observe from Fig. 11 that the benchmark system has the highest MI for each $L$. For the four linear EH based algorithms, the achievable source-destination MI decreases first as $L$ grows and then increases with $L$. The reason is that under a linear EH model, if the relay node is placed nearby the source, more RF energy can be harvested due to a short source-relay distance, which leads to a larger system MI. However, with practical nonlinear EH models, the harvested energy is limited by $E'_m$ when the relay node is very close to the source node. Therefore, for the three proposed algorithms, the achievable MI is lower at $L = 0.25$ than that at $L = 0.6$, as the harvested energy is limited by $E'_m$ at both locations, while the second-hop channel is stronger at $L = 0.6$ than $L = 0.25$. If the relay node is placed nearby the destination node, although the amount of energy harvested at the relay node is reduced because of a longer source-relay distance, a better relay-destination channel thanks to a shorter distance between the relay node and the destination node increases the source-destination MI. We can also see from Fig. 11 that the achievable MI of the proposed method 1 and method 2 is higher than the algorithms in [23], [30], and [29] when $L > 0.75$.

## V. Conclusion

We have investigated the joint source matrix, relay matrix, and PS factor design for a two-hop AF MIMO relay system with a PS-based EH relay node. Compared with the per data stream energy constraints at the relay node adopted by existing approaches, we have proposed a general sum energy constraint at the relay node. A practical nonlinear EH model has been applied at the relay node. The structure of the source and relay precoding matrices has been obtained which reduces the difficult joint transceiver design problem to a simpler joint source and relay power allocation problem. Three methods have been developed to solve the optimal power allocation problem. Simulation examples illustrate that in the linear EH range, the proposed algorithms have a larger system MI than existing PS based AF MIMO relay systems and TS based AF MIMO relay systems with peak transmission power constraints. We have found that the values of the optimal power splitting ratios of subchannels do

not follow the same trend as the source node transmission power increases. Moreover, we have observed that the peak harvest power constraint plays an important role in choosing the location of the relay node. As a future work, it is interesting to study the transceiver optimization of an AF MIMO relay system where the EH relay node is based on the nonlinear diode current analysis model in [40].

## REFERENCES


[1] P. Kamalinejad, C. Mahapatra, Z. Sheng, S. Mirabbasi, V. C. M. Leung, and Y. L. Guan, "Wireless energy harvesting for the Internet of Things," *IEEE Commun. Mag.*, vol. 53, pp. 102–108, Jun. 2015.

[2] X. Zhou, R. Zhang, and C. K. Ho, "Wireless information and power transfer: Architecture design and rate-engergy trade-off," *IEEE Trans. Commun.*, vol. 61, no. 11, pp. 4754–4767, Nov. 2013.

[3] L. R. Varshney, "Transporting information and energy simultaneously," in *Proc. IEEE Int. Symp. Inf. Theory*, Toronto, Canada, Jul. 2008, pp. 1612–1616.

[4] R. Zhang and C. K. Ho, "MIMO broadcasting for simultaneous wireless information and power transfer," *IEEE Trans. Wireless Commun.*, vol. 12, no. 5, pp. 1989–2001, May 2013.

[5] B. Clerckx and E. Bayguzina, "Waveform design for wireless power transfer," *IEEE Trans. Signal Process.*, vol. 64, no. 23, pp. 6313–6328, Dec. 2016.

[6] Y. Zeng, B. Clerckx, and R. Zhang, "Communications and signals design for wireless power transmission," *IEEE Trans. Commun.*, vol. 65, no. 5, pp. 2264–2290, May 2017.

[7] B. Li, C. Z. Wu, H. H. Dam, A. Cantoni, and K. L. Teo, "A parallel low complexity zero-forcing beamformer design for multiuser MIMO systems via a regularized dual decomposition method," *IEEE Trans. Signal Process.*, vol. 63, no. 16, pp. 4179–4190, Aug. 2015.

[8] B. Li, H. H. Dam, A. Cantoni, and K. L. Teo, "A first-order optimal zero-forcing beamformer design for multiuser MIMO systems via a regularized dual accelerated gradient method," *IEEE Commun. Lett.*, vol. 19, no. 2, pp. 195–198, Feb. 2015.

[9] B. Li, Y. Rong, J. Sun, and K. L. Teo, "A distributionally robust linear receiver design for multi-access space-time block coded MIMO systems," *IEEE Trans. Wireless Commun.*, vol. 16, no. 1, pp. 464–474, Jan. 2017.

[10] Q. Shi, L. Liu, W. Xu, and R. Zhang, "Joint transmit beamforming and receieve power splitting for MISO SWIPT," *IEEE Trans. Wireless Commun.*, vol. 13, no. 6, pp. 3269–3280, Jun. 2014.

[11] X. Tang and Y. Hua, "Optimal design of non-regenerative MIMO wireless relays," *IEEE Trans. Wireless Commun.*, vol. 6, no. 4, pp. 1398–1407, Apr. 2007.

[12] Y. Rong, X. Tang, and Y. Hua, "A unified framework for optimizing linear non-regenerative multicarrier MIMO relay communication systmes," *IEEE Trans. Signal Process.*, vol. 6, no. 12, pp. 4837–4851, Dec. 2009.

[13] Y. Rong, "Joint source and relay optimization for two-way linear non-regenerative MIMO relay communications," *IEEE Trans. Signal Process.*, vol. 60, no. 12, pp. 6533–6546, Dec. 2012.

[14] A. A. Nasir, X. Zhou, S. Durrani, and R. A. Kennedy, "Relaying protocols for wireless energy harvesting and information processing," *IEEE Trans. Wireless Commun.*, vol. 12, no. 7, pp. 3622–3636, Jul. 2013.

[15] Z. Ding, S. M. Perlaza, I. Esnaola, and H. V. Poor, "Power allocation strategies in energy harvesting wireless cooperative networks," *IEEE Trans. Wireless Commun.*, vol. 13, no. 2, pp. 846–860, Feb. 2014.

[16] Z. Ding, I. Esnaola, B. Sharif, and H. V. Poor, "Wireless information and power transfer in cooperative networks with spatially random relays," *IEEE Trans. Wireless Commun.*, vol. 13, no. 8, pp. 4400–4453, Aug. 2014.

[17] H. Chen, Y. Li, Y. Jiang, Y. Ma, and B. Vucetic, "Distributed power splitting for SWIPT in relay interference channels using game theory," *IEEE Trans. Wireless Commun.*, vol. 14, no. 1, pp. 410–420, Jan. 2015.

[18] Y. Liu and X. Wang, "Information and energy cooperation in OFDM relaying: Protocols and optimization," *IEEE Trans. Veh. Technol.*, vol. 65, no. 7, pp. 5088–5098, Jul. 2016.

[19] C. Zhong, H. A. Suraweera, G. Zheng, I. Krikidis, and Z. Zhang, "Wireless information and power transfer with full duplex relaying," *IEEE Trans. Commun.*, vol. 62, no. 10, pp. 3447–3461, Oct. 2014.

[20] Z. Wen, X. Liu, N. C. Beaulieu, R. Wang, and S. Wang, "Joint source and relay beamforming design for full-duplex MIMO AF relay SWIPT systems," *IEEE Commun. Lett.*, vol. 20, no. 2, pp. 320–323, Feb. 2016.

[21] H. Liu, K. J. Kim, K. S. Kwak, and H. V. Poor, "Power splitting-based SWIPT with decode-and-forward full-duplex relaying," *IEEE Trans. Wireless Commun.*, vol. 15, no. 11, pp. 3837–3855, Nov. 2016.

[22] Z. Ding *et al.*, "Applications of smart antenna technologies in simultaneous wireless information and power transfer," *IEEE Commun. Mag.*, vol. 53, no. 4, pp. 86–93, Apr. 2015.

[23] K. Xiong, P. Fan, C. Zhang, and K. B. Letaief, "Wireless information and energy transfer for two-hop non-regenerative MIMO-OFDM relay networks," *IEEE J. Select. Areas Commun.*, vol. 26, no. 8, pp. 1397–1407, Aug. 2015.

[24] B. K. Chalise, Y. D. Zhang, and M. G. Amin, "Energy harvesting in an OSTBC based non-regenerative MIMO relay system," in *Proc. IEEE Int. Conf. Acoust., Speech Signal Process.*, Mar. 2012, pp. 3201–3204.

[25] B. K. Chalise, W. K. Ma, Y. D. Zhang, H. Suraweera, and M. G. Amin, "Optimum performance boundaries of OSTBC based AF-MIMO relay system with energy harvesting receiver," *IEEE Trans. Signal Process.*, vol. 61, no. 17, pp. 4199–4213, Sep. 2013.

[26] G. Amarasuriya, E. G. Larsson, and H. V. Poor, "Wireless information and power transfer in multiway massive MIMO relay networks," *IEEE Trans. Wireless Commun.*, vol. 15, no. 6, pp. 3837–3855, Jun. 2016.

[27] Y. Huang and B. Clerckx, "Joint wireless information and power transfer for an autonomous multiple-antenna relay system," *IEEE Commun. Lett.*, vol. 19, no. 7, pp. 1113–1116, Jul. 2015.

[28] Y. Huang and B. Clerckx, "Relaying strategies for wireless-powered MIMO relay networks," *IEEE Trans. Commun.*, vol. 15, no. 9, pp. 6033–6047, Sep. 2016.

[29] J. Liao, M. R. A. Khandaker, and K.-K. Wong, "Energy harvesting enabled MIMO relaying through power splitting," in *Proc. 17th IEEE Int. Workshop Signal Process. Adv. Wireless Commun.*, Edinburgh, Scotland, U.K., Jul. 2016, pp. 1–5.

[30] B. Li and Y. Rong, "Joint transceiver optimization for wireless information and energy transfer in non-regenerative MIMO relay systems," *IEEE Trans. Veh. Technol.*, vol. 67, no. 9, pp. 8348–8362, Sep. 2018.

[31] B. Li and Y. Rong, "AF MIMO relay systems with wireless powered relay node and direct link," *IEEE Trans. Commun.*, vol. 66, no. 4, pp. 1508–1519, Apr. 2018.

[32] B. Li, H. Cao, Y. Rong, T. Su, G. Yang, and Z. He, "Transceiver optimization for DF MIMO relay systems with a wireless powered relay node," *IEEE Access*, vol. 7, pp. 56904–56919, 2019.

[33] E. Boshkovska, D. W. K. Ng, N. Zlatanov, and R. Schober, "Practical non-linear energy harvesting model and resource allocation for SWIPT systems," *IEEE Commun. Lett.*, vol. 19, no. 12, pp. 2082–2085, Dec. 2015.

[34] K. Xiong, B. Wang, and K. J. R. Liu, "Rate-energy region of SWIPT for MIMO broadcasting under nonlinear energy harvesting model," *IEEE Trans. Wireless Commun.*, vol. 16, no. 8, pp. 5147–5161, Aug. 2017.

[35] D. P. Bertsekas, *Nonlinear Programming*. Belmont, MA, USA: Athena Scientific, 1995.

[36] M. Grant and S. Boyd, "The CVX users guide," Release 2.1, Oct. 2014. [Online]. Available: http://web.cvxr.com/cvx/doc/CVX.pdf

[37] J.-M. Kang, I.-M. Kim, and D. I. Kim, "Joint TX power allocation and RX power splitting for SWIPT system with multiple nonlinear energy harvesting circuits," *IEEE Commun. Lett.*, vol. 8, no. 1, pp. 53–56, Feb. 2019.

[38] Y. J. Dong, M. J. Hossain, and J. Cheng, "Performance of wireless powered amplify and forward relaying over Nakagami-$m$ fading channels with nonlinear energy harvester," *IEEE Commun. Lett.*, vol. 20, no. 4, pp. 672–675, Apr. 2016.

[39] L. Shi, L. Zhao, K. Liang, X. Chu, G. Wu, and H.-H. Chen, "Profit maximization in wireless powered communications with improved non-linear energy conversion and storage efficiencies," in *Proc. IEEE Int. Conf. Commun.*, Paris, France, 2017, pp. 1–6.

[40] B. Clerckx, "Wireless information and power transfer: Nonlinearity, waveform design and rate-energy tradeoff," *IEEE Trans. Signal Process.*, vol. 66, no. 4, pp. 847–862, Feb. 2018.

[41] B. Clerckx, R. Zhang, R. Schober, D. W. K. Ng, D. I. Kim, and H. V. Poor, "Fundamentals of wireless information and power transfer: From RF energy harvester models to signal and system designs," *IEEE J. Sel. Areas Commun.*, vol. 37, no. 1, pp. 4–33, Jan. 2019.

[42] B. Clerckx and J. Kim, "On the beneficial roles of fading and transmit diversity in wireless power transfer with nonlinear energy harvesting," *IEEE Trans. Wireless Commun.*, vol. 17, no. 11, pp. 7731–7743, Nov. 2018.

[43] M. Varastehy, B. Rassouli, H. Joudeh, and B. Clerckx, "SWIPT signalling over complex AWGN channels with two nonlinear energy harvester models," in *Proc. IEEE Int. Symp. Inf. Theory*, Vail, CO, USA, Aug. 2018, pp. 866–870.

[44] M. Varastehy, J. Hoydis, and B. Clerckx, "Learning modulation design for SWIPT with nonlinear energy harvester: Large and small signal power regimes," in *Proc. IEEE Int. Workshop Signal Process. Advances Wireless Commun.*, Cannes, France, Jul. 2019, pp. 1–5.
[45] C. R. Valenta and G. D. Durgin, "Harvesting wireless power: Survey of energy-harvester conversion efficiency in far-field, wireless power transfer systems," *IEEE Microw. Mag.*, vol. 15, no. 4, pp. 108–120, Jun. 2014.
[46] T. Le, K. Mayaram, and T. Fiez, "Efficient far-field radio frequency energy harvesting for passively powered sensor networks," *IEEE J. Solid-State Circuits*, vol. 43, no. 5, pp. 1287–1302, May 2008.
[47] J. Guo and X. Zhu, "An improved analytical model for RF-DC conversion efficiency in microwave rectifiers," in *Proc. IEEE MTT-S Int. Microw. Symp. Dig.*, Montreal, QC, Canada, Jun. 2012, pp. 1–3.
[48] M. Varasteh, B. Rassouli, and B. Clerckx, "On capacity-achieving distributions for complex AWGN channels under nonlinear power constraints and their applications to SWIPT," Apr. 2018, *arXiv:1712.01226v2*.
[49] J. Kim, B. Clerckx, and P. D. Mitcheson, "Signal and system design for wireless power transfer: Prototype, experiment and validation," Jan. 2019, *arXiv:1901.01156v1*.
[50] K. W. Choi, D. I. Kim, and M. Y. Chung, "Received power-based channel estimation for energy beamforming in multiple-antenna RF energy transfer system," *IEEE Trans. Signal Process.*, vol. 65, no. 6, pp. 1461–1476, Mar. 2017.
[51] K. Xiong, P. Fan, Y. Lu, and K. B. Letaief, "Energy efficiency with proportional rate fairness in multirelay OFDM networks," *IEEE J. Sel. Areas Commun.*, vol. 34, no. 5, pp. 1431–1447, May 2016.
[52] S. Boyd and L. Vandenberghe, *Convex Optimization*. Cambridge, U.K.: Cambridge Univ. Press, 2004.
[53] M. Stingl, "On the solution of nonlinear semidefinite programs by augmented Lagrangian methods," Ph.D. dissertation, Univ. Erlangen-Nuremberg, Germany, 2006.
[54] Powercaster transmitter, Accessed: Nov. 2018. [Online]. Available: https://www.powercastco.com/products/powercaster-transmitter/
[55] X. Lu, D. Niyato, P. Wang, D. I. Kim, and Z. Han, "Wireless charger networking for mobile devices: Fundamentals, standards, and applications," *IEEE Wireless Commun.*, vol. 22, no. 2, pp. 126–135, Apr. 2015.
[56] C. Song, J. Park, B. Clerckx, I. Lee, and K.-J. Lee, "Generalized precoder designs based on weighted MMSE criterion for energy harvesting constrained MIMO and multi-user MIMO channels," *IEEE Trans. Wireless Commun.*, vol. 15, no. 12, pp. 7941–7954, Dec. 2016.

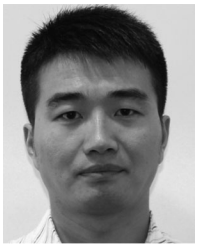

**Bin Li** (M'18–SM'18) received the bachelor's degree in automation and the master's degree in control science and engineering from the Harbin Institute of Technology, Harbin, China, in 2005 and 2008, respectively, and the Ph.D. degree in mathematics and statistics from Curtin University, Perth, WA, Australia, in 2011. From 2012–2014, he was a Research Associate with the School of Electrical, Electronic and Computer Engineering, the University of Western Australia, Perth, WA, Australia. From 2014–2017, he was a Research Fellow with the Department of Mathematics and Statistics, Curtin University. He is currently a Research Professor with the School of Electrical Engineering and Information, Sichuan University, Chengdu, China. His research interests include signal processing, wireless communications, optimization, and optimal control.

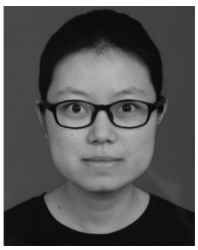

**Meiying Zhang** received the bachelor's degree in electrical engineering and automation from the University of Jinan, China, in 2014. She is currently working toward the master's degree in control theory and control engineering from the College of Electrical Engineering, Sichuan University, China. Her research interests include signal processing and wireless communications.

**Hanyu Cao** received the bachelor's degree in instrument engineering from Sichuan University. He is currently working toward the master's degree in control science from Sichuan University, since 2017. His research interests include signal processing, wireless communications, optimization and optimal control.

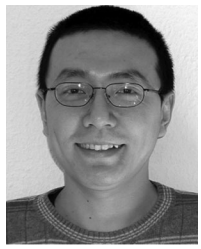

**Yue Rong** (S'03–M'06–SM'11) received the Ph.D. degree (*summa cum laude*) in electrical engineering from the Darmstadt University of Technology, Darmstadt, Germany, in 2005. He was a Postdoctoral Researcher with the Department of Electrical Engineering, University of California, Riverside, from February 2006 to November 2007. Since December 2007, he has been with Curtin University, Bentley, Australia, where he is currently a Professor. His research interests include signal processing for communications, wireless communications, underwater acoustic communications, underwater optical wireless communications, applications of linear algebra and optimization methods, and statistical and array signal processing. He has published over 160 journal and conference papers in these areas. Dr. Rong was a recipient of the Best Paper Award at the 2011 International Conference on Wireless Communications and Signal Processing, the Best Paper Award at the 2010 Asia-Pacific Conference on Communications, and the Young Researcher of the Year Award of the Faculty of Science and Engineering at Curtin University in 2010. He was an Associate Editor of the IEEE TRANSACTIONS ON SIGNAL PROCESSING from 2014 to 2018, an Editor of the IEEE WIRELESS COMMUNICATIONS LETTERS from 2012 to 2014, and a Guest Editor of the IEEE JOURNAL ON SELECTED AREAS IN COMMUNICATIONS Special Issue on Theories and Methods for Advanced Wireless Relays. He was also a TPC Member for the IEEE ICC, IEEE GlobalSIP, EUSIPCO, IEEE ICCC, WCSP, IWCMC, and ChinaCom.

**Zhu Han** (S'01–M'04–SM'09–F'14) received the B.S. degree in electronic engineering from Tsinghua University, in 1997, and the M.S. and Ph.D. degrees in electrical and computer engineering from the University of Maryland, College Park, in 1999 and 2003, respectively. From 2000 to 2002, he was an R&D Engineer of JDSU, Germantown, Maryland. From 2003 to 2006, he was a Research Associate with the University of Maryland. From 2006 to 2008, he was an Assistant Professor with Boise State University, Idaho. Currently, he is a John and Rebecca Moores Professor with the Electrical and Computer Engineering Department as well as in the Computer Science Department at the University of Houston, Texas. He is also a Chair Professor with National Chiao Tung University, ROC. His research interests include wireless resource allocation and management, wireless communications and networking, game theory, big data analysis, security, and smart grid. Dr. Han received an NSF Career Award in 2010, the Fred W. Ellersick Prize of the IEEE Communication Society in 2011, the EURASIP Best Paper Award for the *Journal on Advances in Signal Processing* in 2015, IEEE Leonard G. Abraham Prize in the field of communications systems (Best Paper Award in IEEE JSAC) in 2016, and several best paper awards in IEEE conferences. He was an IEEE Communications Society Distinguished Lecturer from 2015–2018, and is AAAS Fellow since 2019 and ACM Distinguished Member since 2019. He is 1% highly cited researcher since 2017 according to Web of Science.